Contribution from the Department of Chemistry, University of Virginia, Charlottesville, Virginia 22901

Magnetic Circularly Polarized Luminescence Spectra of 9-Coordinate Europium(III) Complexes in Aqueous Solution

DAVID R. FOSTER and F. S. RICHARDSON*

Received January 14, 1983

Unpolarized emission spectra and magnetic field induced circularly polarized emission spectra are reported for four different Eu^{3+}/ligand systems in aqueous solution at pH ≥8 and with $[Eu^{3+}]/[ligand] \leq 0.33$. Under these solution conditions, each of the ligands is expected to coordinate to Eu^{3+} via a terdentate chelation mode, forming 9-coordinate tris-terdentate complexes. The ligands are oxydiacetate (ODA), dipicolinate (DPA), iminodiacetate (IDA), and (methylimino)diacetate (MIDA). The polarized emission results reveal that the dominant coordination species formed in the 1:3 Eu^{3+}/ODA and 1:3 Eu^{3+}/DPA systems are tris-terdentate $Eu(ligand)_3^{3-}$ complexes having trigonal dihedral (D_3) symmetry. For the 1:5 Eu^{3+}/MIDA system, the polarized emission results suggest $Eu(MIDA)_3^{3-}$ complexes of C_{3h} symmetry as the dominant coordination species present in solution. The spectra obtained for the Eu^{3+}/IDA system indicate that the dominant coordination species have nonaxially symmetric structures. The latter are attributed to outer-sphere complexes formed via interactions between bound >N–H groups and unbound IDA molecules in solution. Although the unpolarized emission spectra obtained for the various Eu^{3+}/ligand systems exhibit some sensitivity to the ligand environment (especially the $^7F_2 \leftarrow {}^5D_0$ intensities and the $^7F_1 \leftarrow {}^5D_0$ crystal field splittings), the magnetic field induced circularly polarized emission spectra are shown to be considerably more useful for eliciting structural information about the complexes.

Introduction

The $^7F_J \leftarrow {}^5D_0$ emission spectra of europium(III) complexes provide especially useful probes of ligand structure and ligand field symmetry. The $^5D_0$ emitting state is nondegenerate and is always totally symmetric in the point group of the Eu(III) coordination site. The $^7F_0$ ground multiplet level is also nondegenerate and totally symmetric, so that the $^7F_0 \leftarrow {}^5D_0$ transition must always consist of just one line whose intensity (or appearance) is subject to rather strict symmetry conditions. The $^7F_1$ multiplet can split, at most, into just three components in the presence of a ligand field or an externally applied magnetic field, and the dominant mechanism for a $^7F_1 \leftarrow {}^5D_0$ radiative transition in Eu(III) systems is known to be magnetic dipole. This transition is magnetic dipole allowed in the "free ion" (by the intermediate-coupling selection rule, $\Delta J = 0, \pm 1$, excluding $J = J' = 0$), so that its oscillator strength is expected to be relatively independent of the ligand environment. However, the splitting pattern and intensity distribution *within* a $^7F_1 \leftarrow {}^5D_0$ transition region can provide detailed information about ligand field strength and symmetry.

The $^7F_2 \leftarrow {}^5D_0$ transition can exhibit, at most, five crystal field sublevels (or five Zeeman sublevels in an externally applied magnetic field), so that its interpretation with regard to structural perturbations on the Eu(III) ion remains relatively uncomplicated. However, the major interest in this transition as a structure probe derives from its *hypersensitive* behavior. That is, the oscillator strength of this transition is known to be extraordinarily sensitive to the details of the ligand environment about the Eu(III) ion.[1-5] The dominant intensity mechanism for the $^7F_2 \leftarrow {}^5D_0$ transition is electric dipole, and the ligand field plays the *essential* role of providing a noncentrosymmetric potential (static or dynamic) to break parity conservation in the $4f \rightarrow 4f$ transition processes. The splitting patterns and intensity distributions become progressively more complicated in the $^7F_{3,4,5,6} \leftarrow {}^5D_0$ transitions, and spectra–structure correlations become more difficult to sort out.

In a previous paper[6] we demonstrated the utility of $^7F_{0,1,2} \leftarrow {}^5D_0$ magnetic circularly polarized luminescence (MCPL) spectra for deducing structural information about europium(III) complexes in solution media. MCPL is the emission analogue of magnetic circular dichroism (MCD), and its theory and applications have been discussed in detail elsewhere.[7,8] In the MCPL experiment, a static magnetic field is applied to the sample with the magnetic field direction aligned parallel to the direction of emission collection and detection. Application of the magnetic field in this configuration will cause the sample to emit light that is elliptically polarized (that is, unequal amounts of left and right circularly polarized light). The emitted light is analyzed in terms of a circular intensity differential, $\Delta I = I_L - I_R$, and in terms of total intensity, $I = I_L + I_R$, where $I_{L(R)}$ denotes the intensity of the left (right) circularly polarized component of the emitted light. Since ΔI is a signed quantity whereas I is not, it may be expected that two closely spaced, strongly overlapping emission bands that remain unresolved in the total emission spectrum (I vs. λ) may be clearly resolved in the MCPL spectrum (ΔI vs. λ) if they have oppositely signed ΔI values. Therefore, at the very least, one may expect MCPL measurements to aid the detection of slightly split components within the $^7F_{J>0} \leftarrow {}^5D_0$ emission manifolds of Eu(III) systems.

In the present study, we report unpolarized emission and MCPL spectra obtained on four different europium(III) complexes in aqueous solution and show how these spectra can be used to deduce structural information about the complexes. The ligands used in forming these complexes were oxydiacetate (**1**), dipicolinate (**2**), iminodiacetate (**3**), and (methylimino)diacetate (**4**). Each of these ligands is potentially terdentate with respect to chelation to a metal ion (forming two five-membered chelate rings), and each has two carboxylate donor groups in terminal positions. However, they each differ with respect to their middle donor moiety. In **1**, this moiety is an ether oxygen atom; in **2**, this moiety is a pyridinium nitrogen atom; in **3**, this moiety is a secondary amine nitrogen atom; and in **4**, this moiety is a tertiary amine nitrogen atom. They also differ with respect to the conformational properties predicted for their chelate ring systems. For **1** and **2**, one predicts that the two chelate rings formed in terdentate binding should be nearly coplanar. This prediction is based on the sp^2-type of orbital hybridization characteristic of the middle donor atoms in these two ligands and is supported by X-ray crystallographic data on lanthanide complexes of **1**[9,10] and **2**.[11-14]

(1) Peacock, R. D. *Struct. Bonding (Berlin)* **1975**, *22*, 83.
(2) Henrie, D. E.; Fellows, R. L.; Choppin, G. R. *Coord. Chem. Rev.* **1976**, *18*, 199.
(3) Richardson, F. S.; Saxe, J. D.; Davis, S. A.; Faulkner, T. R. *Mol. Phys.* **1981**, *42*, 1401.
(4) Kirby, A. F.; Richardson, F. S. *J. Phys. Chem.* **1983**, *87*, 2544, 2557.
(5) Kirby, A. F.; Foster, D.; Richardson, F. S. *Chem. Phys. Lett.* **1983**, *95*, 507.
(6) Richardson, F. S.; Brittain, H. G. *J. Am. Chem. Soc.* **1981**, *103*, 18.
(7) Riehl, J. P.; Richardson, F. S. *J. Chem. Phys.* **1977**, *66*, 1988.
(8) Richardson, F. S.; Riehl, J. P. *Chem. Rev.* **1977**, *77*, 773.
(9) Albertsson, J. *Acta Chem. Scand.* **1968**, *22*, 1563.
(10) Albertsson, J. *Acta Chem. Scand.* **1970**, *24*, 3527.
(11) Albertsson, J. *Acta Chem. Scand.* **1970**, *24*, 1213.

0020-1669/83/1322-3996$01.50/0

For **3** and **4**, one predicts that the two chelate rings formed upon binding will be noncoplanar. This prediction is based on the sp^3-type of orbital hybridization characteristic of amine nitrogen atoms, and this prediction is also supported by X-ray crystallographic data.[15]

9-Coordinate tris-terdentate lanthanide(III) complexes of **1** and **2** have been crystallized and structurally characterized (in the solid state).[9-14] For each, the coordination polyhedron (LnL_9) was found to be a slightly distorted tricapped trigonal prism with the lanthanide ion at a site of exact D_3 symmetry. Carboxylate donor atoms form the top and bottom triangles of the prism, and the equatorial sites are occupied by the middle donor atoms of the respective ligands. In each case, the terdentate ligands stretch *diagonally* across the rectangular faces of the tricapped trigonal prism in the so-called meridional (or *mer*) isomeric form (see Figure 15 of Favas and Kepert[16]).

There have been no reports of tris-terdentate lanthanide(III) complexes of **3** and **4** being isolated or crystallized. There is, however, some evidence that such complexes do exist as the majority species in aqueous solution at pH >8 when the [ligand]:[Ln^{3+}] concentration ratio exceeds a value of 3.[17-19] This evidence is based on potentiometric titration[17] and spectroscopic data.[18,19] Furthermore, it has been suggested[19] that the coordination polyhedron of these complexes also has a tricapped trigonal-prismatic structure. However, in these systems the ligands would wrap around the prism in a facial (or *fac*) isomeric form (see Figure 15 of Favas and Kepert[16]), giving the overall structure C_{3h} symmetry.

All of the spectra reported in the present study were obtained on aqueous solution samples under conditions in which tris-terdentate chelation would be favored. [Eu^{3+}]:[ligand] concentration ratios were either 1:3 or 1:5, and solution pH was maintained in the 8–9 range. Under these conditions, the *majority* species in solution would be expected to be Eu(ligand)$_3^{3-}$.

Although the principal objective of this study is to elucidate the structural properties of the ligand environment about the Eu(III) ion, there is also a secondary objective to examine how differences in the ligand environment serve to modulate the *relative* intensities of the $^7F_J \leftarrow {}^5D_0$ emissions.

Theory

Here we shall sketch those aspects of MCPL theory and lanthanide crystal field theory that are most relevant to analyzing the data obtained in the present study. The 4f-electron Hamiltonian of a lanthanide complex subjected to an externally applied (static) magnetic field can be written as

$$H_{4f} = H_{4f}^0 + H_{cf}^+ + H_{cf}^- + H_{ze} \tag{1}$$

where H_{4f}^0 is the Hamiltonian for the 4f electrons in the "free ion", H_{cf}^+ represents the even-parity components of the crystal field Hamiltonian, H_{cf}^- represents the odd-parity components of the crystal field Hamiltonian, and H_{ze} is the Zeeman operator. The eigenstates of H_{4f}^0 are taken to be the 4f-electron intermediate-coupling states $|4f^N\psi[SL]JM_J\rangle$. We shall consider H_{cf}^+ to operate only *within* this manifold of states and shall define this operator as

$$H_{cf}^+ = \sum_{k,q} B_q^{(k)} U_q^{(k)} = \sum_{k,q} h^+(k,q) \tag{2}$$

where $k = 2$, 4, and 6, q is a projection of k on the axis of quantization, and $U_q^{(k)}$ is the intraconfigurational unit tensor operator.[20] The $B_q^{(k)}$ in eq 2 are the even-parity crystal field coefficients of the system. In general, H_{cf}^+ will be off-diagonal with respect to both J and M_J, leading to crystal field states of mixed J and M_J parentage.

The H_{cf}^- operator represents all 4f-electron/ligand interactions having odd parity. To first order, it is an *inter*configurational operator that serves to mix the even-parity 4f-electron states with odd-parity states of the system (which may or may not be localized on the lanthanide ion). This operator is responsible for all the electric dipole intensity associated with the 4f → 4f transitions. The Zeeman operator is defined by

$$H_{ze} = \mu_B \mathbf{B}\cdot(\mathbf{L} + 2\mathbf{S}) \tag{3}$$

where μ_B is the Bohr magneton, **B** is the applied magnetic field strength vector, and **L** and **S** are respectively the orbital and spin angular momentum vector operators. When an axis of quantization is chosen parallel to **B**, the H_{ze} operator is diagonal with respect to M_J with eigenvalues $M_J g \mu_B |\mathbf{B}|$, where g is the gyromagnetic factor for (in our case) a 4f electron.

Detailed consideration of the H_{cf}^- operator is essential to rationalizing the electric dipole intensities of the $^7F_J \leftarrow {}^5D_0$ transitions in terms of ligand field effects. To first order in H_{cf}^- and with all J–J' mixings ignored, the intermediate-coupling selection rules governing $^7F_J \leftarrow {}^5D_0$ electric dipole strengths are $\Delta J = 2$, 4, or 6. The $^7F_{0,1,3,5} \leftarrow {}^5D_0$ transitions can acquire electric dipole strength only to second order—first order in H_{cf}^- *plus* first order in H_{cf}^+ (leading to J–J′ mixings). Quantitative treatments of 4f → 4f electric dipole strengths are made difficult by the lack of any direct, empirically based methods for accurately parameterizing the H_{cf}^- operator and by the necessity for dealing with sets of ill-defined odd-parity states.[1] In the present study, we shall avoid these problems by focusing our attention primarily on the $^7F_1 \leftarrow {}^5D_0$ transition, whose intensity is due almost entirely to a magnetic dipole mechanism. In this case, the H_{cf}^- operator can be ignored to first order, and the H_{cf}^+ and H_{ze} operators can be treated as perturbations on H_{4f}^0..

The most important components of H_{cf}^+ with respect to their influence on the $^7F_1 \leftarrow {}^5D_0$ transition are those with $k = 2$. The principal effects of these components are to split and/or mix the $M_J = 0, \pm 1$ sublevels of the $^7F_1$ multiplet. We define, therefore, an "effective" H_{cf}^+ operator for the $J = 1$ multiplet as

$$H_{cf}^+(J = 1) \equiv H_{cf}^+(1) = h^+(2,0) + h^+(2,1) + h^+(2,2) \tag{4}$$

where each of the $h^+(k,q)$ operators is assumed to include both the + and − components of q (see eq 2 for how these operators are defined). The $h^+(2,0)$ operator is diagonal in M_J, the $h^+(2,1)$ operator mixes M_J levels according to $|\Delta M_J| = 1$, and the $h^+(2,2)$ operator mixes M_J levels according to $|\Delta M_J| = 2$.

For all axially symmetric systems (i.e., systems having at least one C_n symmetry element with $n > 2$), the $h^+(2,1)$ and $h^+(2,2)$ operators are identically zero. However, for most (but not all) axially symmetric systems, the $h^+(2,0)$ operator does *not* vanish by symmetry. For example, $h^+(2,0)$ is symmetry allowed in systems having D_{3h}, D_3, C_{3h}, C_{3v}, or C_3 point-group symmetry. *Within* a $J = 1$ multiplet, the effect of $h^+(2,0)$ is to split the multiplet into two sublevels, one of which is nondegenerate and corresponds to $M_J = 0$ and the other of which is 2-fold degenerate and corresponds to $M_J = \pm 1$. The energies of these two sublevels can be expressed, to first order in $h^+(2,0)$, as

$$E_{1,0} = E_1^0 + \Delta_1(2,0) \tag{5}$$

$$E_{1,\pm 1} = E_1^0 - (1/2)\Delta_1(2,0) \tag{6}$$

(12) Albertsson, J. *Acta Chem. Scand.* **1972**, *26*, 985.
(13) Albertsson, J. *Acta Chem. Scand.* **1972**, *26*, 1005.
(14) Albertsson, J. *Acta Chem. Scand.* **1972**, *26*, 1023.
(15) Oskarsson, A. *Acta Chem. Scand.* **1971**, *25*, 1206.
(16) Favas, M. C.; Kepert, D. L. *Prog. Inorg. Chem.* **1981**, *28*, 309.
(17) Grenthe, I.; Gardhammar, G. *Acta Chem. Scand.* **1971**, *25*, 1401.
(18) Salama, S.; Richardson, F. S. *J. Phys. Chem.* **1980**, *84*, 512.
(19) Davis, S. A. Ph.D. Dissertation, University of Virginia, 1981.
(20) Wybourne, B. G. "Spectroscopic Properties of Rare Earths"; Wiley-Interscience: New York, 1965.

where E_1^0 denotes the energy of the unperturbed ("free-ion") multiplet level, and $\Delta_1(2,0) = \{4f^N\psi[SL]JM_J|h^+(2,0)|4f^N\psi[SL]JM_J\}$ with $J = 1$ and $M_J = 0$. Application of a magnetic field to this system will split the $M_J = \pm1$ state into its Zeeman sublevels. Therefore, to first order in $h^+(2,0)$ *and* H_{ze}, we have

$$E'_{1,0} = E_{1,0} = E_1^0 + \Delta_1(2,0) \quad (7)$$

$$E'_{1,\pm1} = E_1^0 - \tfrac{1}{2}\Delta_1(2,0) \pm g\mu_B|\mathbf{B}| \quad (8)$$

For nonaxially symmetric systems in which either one or both of the $h^+(2,1)$ and $h^+(2,2)$ operators are nonvanishing, the splitting patterns within the $J = 1$ multiplet can become significantly more complicated to interpret. Under these conditions, the sublevels can no longer be characterized in terms of well-defined M_J quantum numbers, even when crystal field induced J–J' mixings are ignored. That is, both $h^+(2,1)$ and $h^+(2,2)$ are off-diagonal with respect to M_J. A detailed account of how the $h^+(2,1)$ and $h^+(2,2)$ operators can affect the energy levels and wave functions of a $J = 1$ multiplet has been given in ref 6.

Now let us consider the total (unpolarized) emission intensity (I) and the differential (left minus right) circularly polarized emission intensity (ΔI) associated with the $^7F_1 \leftarrow {}^5D_0$ transition for an assembly of randomly oriented systems in which $H^+_{cf}(1) = h^+(2,0)$. We shall assume a magnetic dipole radiative mechanism for this transition and shall assume that both $h^+(2,0)$ and H_{ze} operate only *within* the $^7F_1$ multiplet. To first order, H_{ze} will lift the degeneracy of the $\pm1 \leftarrow 0$ ($^7F_{1,\pm1} \leftarrow {}^5D_0$) transitions and will mix each of the $M_J = \pm1$ levels with the $M_J = 0$ level (within the $^7F_1$ multiplet). On the assumption that $|2g\mu_B\mathbf{B}|$ is smaller than the half-width of the zero-field $\pm1 \leftarrow 0$ emission band, the total emission spectrum (I vs. E) within the $\pm1 \leftarrow 0$ transition region is given by

$$I/E = K\nu_{10}^3\, \bar{D}_0(1\leftarrow0)\, f_{10}(E) \quad (9)$$

where E denotes photon energy, ν_{10} is the $\pm1 \leftarrow 0$ transition frequency at zero field, $f_{10}(E)$ is a normalized line shape function centered at ν_{10}, and $\bar{D}_0(1\leftarrow0)$ is a magnetic dipole strength defined by

$$\bar{D}_0(1\leftarrow0) = \tfrac{1}{3}[|\langle{}^7F_{1,1}|\mathbf{m}|{}^5D_0\rangle|^2 + |\langle{}^7F_{1,-1}|\mathbf{m}|{}^5D_0\rangle|^2] \quad (10)$$

Within the $0 \leftarrow 0$ ($^7F_{1,0} \leftarrow {}^5D_0$) transition region, we have

$$I/E = K\nu_{00}^3\, \bar{D}_0(0\leftarrow0)\, f_{00}(E) \quad (11)$$

where $\bar{D}_0(0\leftarrow0) = {}^1/_3|\langle{}^7F_{1,0}|\mathbf{m}|{}^5D_0\rangle|^2$, and $f_{00}(E)$ is a line-shape function centered at the $0 \leftarrow 0$ transition frequency, ν_{00}. The magnetic dipole operator is denoted by $\mathbf{m}$, and $K = 8\pi^3N_e/c^3$, where N_e denotes the emitting-state ($^5D_0$) population under steady-state irradiation conditions.

The MCPL (ΔI) spectrum within the $\pm1 \leftarrow 0$ transition region may be expressed as

$$\Delta I/E = -K\nu_{10}^3\mu_B|\mathbf{B}|[\bar{A}_1(1\leftarrow0)\, f'_{10}(E) + \bar{B}_0(1\leftarrow0)\, f_{10}(E)] \quad (12)$$

and within the $0 \leftarrow 0$ transition region as

$$\Delta I/E = -K\nu_{00}^3\mu_B|\mathbf{B}|\bar{B}_0(0\leftarrow0)\, f_{00}(E) \quad (13)$$

where $f'_{10} = \partial f_{10}/\partial E$ and K is defined as in eq 9 and 11. $\bar{A}_1$ and $\bar{B}_0$ are orientationally averaged magnetooptical Faraday parameters[7] defined, in the present case, by

$$\bar{A}_1(1\leftarrow0) = -(i/3\mu_B)\sum_{\lambda,\lambda'}[\langle{}^7F_{1,\lambda}|\mathbf{m}|{}^7F_{1,\lambda'}\rangle \cdot \langle{}^5D_0|\mathbf{m}|{}^7F_{1,\lambda}\rangle \times \langle{}^7F_{1,\lambda'}|\mathbf{m}|{}^5D_0\rangle] \quad (14)$$

$$\bar{B}_0(0\leftarrow0) = -\bar{B}_0(1\leftarrow0) = (8/9\mu_B\Delta_1)\mathrm{Im}[\langle{}^7F_{1,0}|\mathbf{m}|{}^7F_{1,1}\rangle \cdot \langle{}^5D_0|\mathbf{m}|{}^7F_{1,0}\rangle \times \langle{}^7F_{1,1}|\mathbf{m}|{}^5D_0\rangle] \quad (15)$$

where λ and λ' in eq 14 run over $M_J = \pm1$ (of the $^7F_1$ multiplet), and Δ_1 is the crystal field energy parameter appearing in eq 5–8. In terms of zero-field transition frequencies, $\Delta_1 = (2h/3)(\nu_{10} - \nu_{00})$. The matrix elements in eq 14 and 15 are over *zero-field* state functions. To first order in $h^+(2,0)$ and H_{ze} (and neglecting all J–J' mixings), the *overall* MCPL spectrum in the $^7F_1 \leftarrow {}^5D_0$ transition region may now be expressed as

$$\Delta I/E = -K\mu_B|\mathbf{B}|\{\bar{A}_1(1\leftarrow0)\ \nu_{10}^3 f'_{10}(E) + \bar{B}_0(1\leftarrow0)[\nu_{10}^3 f_{10}(E) - \nu_{00}^3 f_{00}(E)]\} \quad (16)$$

The A term in eq 16 arises from the field-induced Zeeman splitting of the M_J multiplet, and the B terms arise from field-induced mixings between the $M_J = 0$ and ±1 sublevels. Note that $\int(\Delta I/E)\,dE = -K\mu_B|\mathbf{B}|\bar{B}_0(1\leftarrow0)[\nu_{10}^3 - \nu_{00}^3]$.

The tris-terdentate complexes of **1** and **2** are predicted to have D_3 symmetry, and the tris-terdentate complexes of **3** and **4** are expected to have C_{3h} symmetry. Therefore, if tris-terdentate chelation represents the dominant structural form for the complexes of these ligands (with Eu^{3+} ions) under neutral to slightly basic pH conditions, one can expect to observe the simple $^7F_1 \leftarrow {}^5D_0$ MCPL behavior described above. However, it is unlikely that any of the other structural types of complexes possibly formed by these ligands will have axial symmetry. If these other structural types (e.g., bis complexes or complexes involving only bidentate chelation) are present in any significant concentration, then one may expect a somewhat more complicated $^7F_1 \leftarrow {}^5D_0$ MCPL spectrum.

Detailed MCPL analysis within the $^7F_2 \leftarrow {}^5D_0$ transition region of Eu(III) complexes requires the introduction of electric dipole intensity parameters. However, in this transition region differentiation between complexes of D_3 and C_{3h} symmetries is made simple by the relevant dipole selection rules for radiative processes. In D_3 symmetry, one expects to observe two electric dipole transitions, $E_a \leftarrow A_1$, having *mixed* $\Delta M_J = \pm1$ and $\Delta M_J = \pm2$ character (the $M_J = \pm1$ and ±2 sublevels of the $^7F_2$ multiplet will be mixed by the $h^+(4,3)$ component of the D_3 crystal field potential). In C_{3h} symmetry, however, one expects to observe just one electric dipole transition, $E' \leftarrow A'$, which has pure $\Delta M_J = \pm2$ character. In D_3 symmetry, both $E_a \leftarrow A_1$ and $E_b \leftarrow A_1$ are also magnetic dipole allowed. In C_{3h} symmetry, $E' \leftarrow A'$ is magnetic dipole forbidden, but one has two additional transitions, $A' \leftarrow A'$ ($\Delta M_J = 0$) and $E'' \leftarrow A'$ ($\Delta M_J = \pm1$), which are magnetic dipole allowed.

The signs of the Faraday A terms observed in the $^7F_2 \leftarrow {}^5D_0$ MCPL spectra will reflect the $\Delta M_J = \pm1$ or ±2 compositions of the erstwhile (zero-field) doubly degenerate $E \leftarrow A$ crystal field transitions. For $\Delta M_J = \pm1$, the sign of the A term will be identical with that observed in the $^7F_1 \leftarrow {}^5D_0$ transition region (see eq 16 above). For $\Delta M_J = \pm2$, the sign of the A term will be opposite that observed in the $^7F_1 \leftarrow {}^5D_0$ spectrum. On the assumption that the E_a and E_b states in D_3 symmetry have *unequal* amounts of $M_J = \pm1$ vs. $M_J = \pm2$ character, one may anticipate oppositely signed Faraday A terms for the $E_a \leftarrow A_1$ and $E_b \leftarrow A_1$ crystal field transitions in the $^7F_2 \leftarrow {}^5D_0$ MCPL spectra. In C_{3h} symmetry, the electric dipole allowed $E' \leftarrow A'$ transition should exhibit a Faraday A term *opposite* in sign to that observed in the $^7F_1 \leftarrow {}^5D_0$ transition region, whereas the magnetic dipole allowed $E'' \leftarrow A'$ transition (expected to be much weaker than the $E' \leftarrow A'$ transition) should exhibit a Faraday A term *identical* in sign with that observed in the $^7F_1 \leftarrow {}^5D_0$ MCPL spectrum.

Each of the crystal field transitions in the $^7F_2 \leftarrow {}^5D_0$ emission region will also exhibit Faraday B terms in the MCPL spectra. However, to determine the relative signs and magnitudes of these terms would require that *both* the $h^+(2,q)$ and $h^+(4,q)$ crystal field components be known. We do not pursue this problem in the present study.

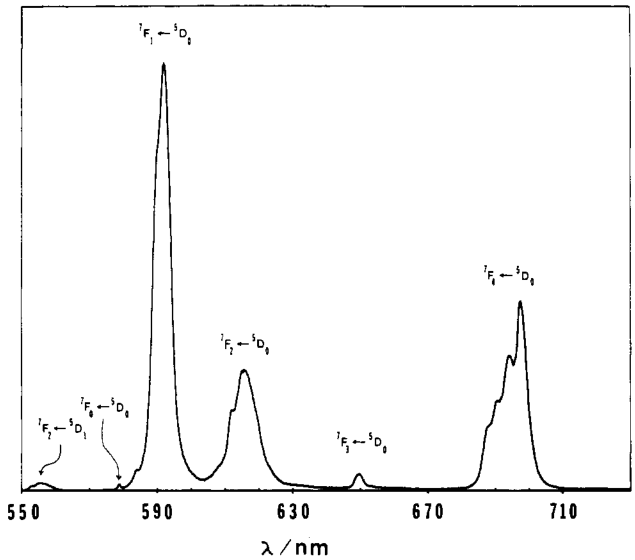

Figure 1. Unpolarized emission spectrum for 0.10 M $EuCl_3$ in water at pH ~6.5 (λ_{ex} = 395 nm, $\Delta\lambda_{em}$ = 0.5 nm; no magnetic field).

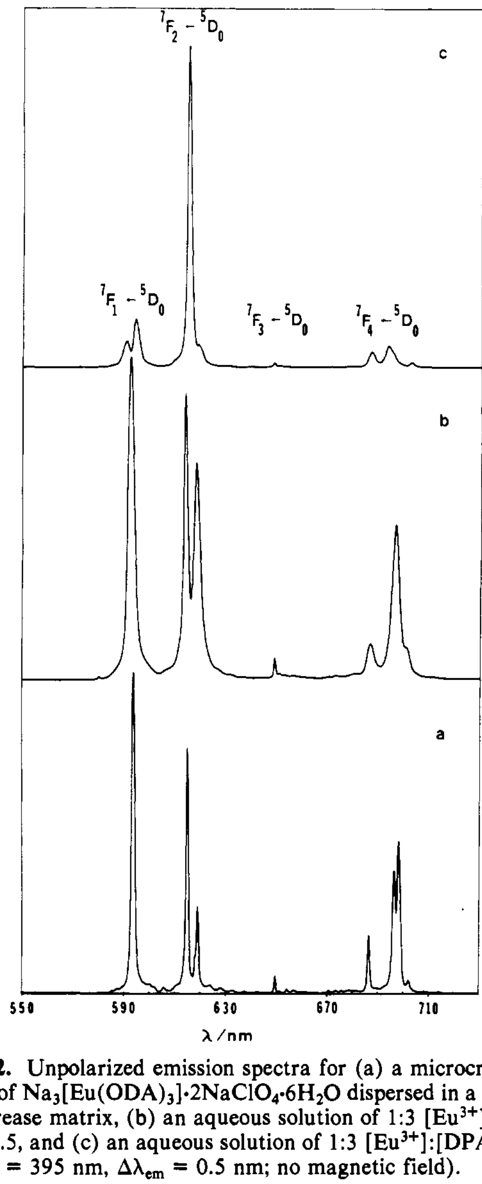

Figure 2. Unpolarized emission spectra for (a) a microcrystalline sample of $Na_3[Eu(ODA)_3]\cdot 2NaClO_4\cdot 6H_2O$ dispersed in a KBr/silicone grease matrix, (b) an aqueous solution of 1:3 [Eu^{3+}]:[ODA] at pH 8.5, and (c) an aqueous solution of 1:3 [Eu^{3+}]:[DPA] at pH 8.5 (λ_{ex} = 395 nm, $\Delta\lambda_{em}$ = 0.5 nm; no magnetic field).

Experimental Section

The ligands **1** (oxydiacetate, or ODA), **2** (dipicolinate, or DPA), **3** (iminodiacetate, or IDA), and **4** ((methylimino)diacetate, or MIDA) were each purchased from Aldrich in their diacid form. $EuCl_3\cdot 6H_2O$ (99.9% purity) was also purchased from Aldrich. All spectroscopic measurements were carried out on aqueous solutions in which the pH was adjusted between 8.0 and 9.5. For ODA (**1**) and DPA (**2**), the [Eu^{3+}]:[ligand] concentration ratio was fixed at 1:3. For IDA (**3**) and MIDA (**4**), the [Eu^{3+}]:[ligand] concentration ratio was fixed at 1:5. Measurements were carried out on samples with [Eu^{3+}] = 0.01 M and also on samples with [Eu^{3+}] = 0.10 M. The results obtained at these two concentrations were *qualitatively* identical.

Medium-resolution ($\Delta\lambda$ ~ 0.5 nm) excitation and emission spectra (unpolarized) were obtained on an SLM Model 8000 photon-counting emission spectrophotometer. This instrument has a 450-W xenon arc lamp for a light source, and it records *corrected* excitation and emission spectra. All emission spectra recorded with this instrument were obtained with broad-band excitation centered at 395 nm.

The MCPL experiments were carried out with the samples contained in an insulated cell placed in the bore of a superconducting magnet (Oxford Instruments). Sample temperature was maintained at ~296 K in all experiments. Sample luminescence was excited with the 466-nm line of a CW argon ion laser (corresponding to $^7F_0 \rightarrow {}^5D_2$ Eu(III) absorption), and the MCPL and total luminescence (TL) spectra were recorded simultaneously on an emission spectrophotometer constructed in this laboratory.[8] Magnetic field strengths were varied between 0 and 4.2 T. All MCPL spectra are displayed as ΔI vs. $\bar{\nu}$ (cm^{-1}) plots, where $\Delta I = I_L - I_R$. All total luminescence spectra are displayed as $I/2$ vs. $\bar{\nu}$ (cm^{-1}) plots, where $I = I_L + I_R$. Both ΔI and I are scaled in arbitrary units.

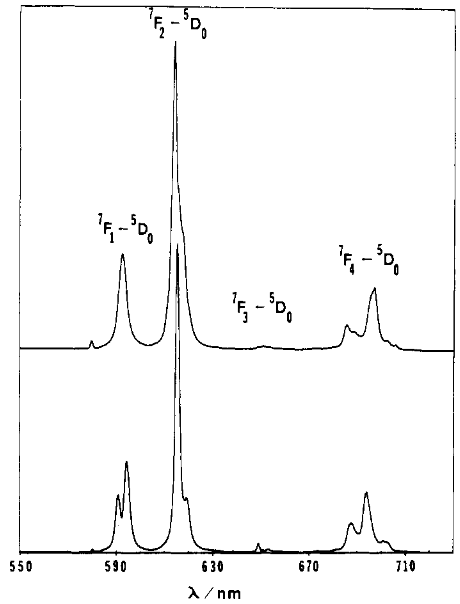

Figure 3. Unpolarized emission spectra for aqueous solutions of 1:5 [Eu^{3+}]:[MIDA] (top) and 1:5 [Eu^{3+}]:[IDA] (bottom) at pH ~8.5–9.0 (λ_{ex} = 395 nm, $\Delta\lambda_{em}$ = 0.5 nm; no magnetic field).

Results

Unpolarized Emission Spectra. Unpolarized emission spectra obtained in the *absence* of an applied magnetic field are shown in Figures 1–3. The spectrum shown in Figure 1 is that of 0.10 M $EuCl_3$ in water at pH ~6.5. Of special note in this spectrum are (1) the dominance of the $^7F_1 \leftarrow {}^5D_0$ emission and (2) the greater intensity of the $^7F_4 \leftarrow {}^5D_0$ emission relative to that of the $^7F_2 \leftarrow {}^5D_0$ emission. The spectrum shown in Figure 2a is that obtained on microcrystalline samples of $Na_3[Eu(ODA)_3]\cdot 2NaClO_4\cdot 6H_2O$ dispersed in a KBr/silicone grease matrix. The spectrum shown in Figure 2b is that obtained for a 1:3 [Eu^{3+}]:[ODA] aqueous solution sample with [Eu^{3+}] = 0.10 M and pH = 8.5. Except for some line broadening in the solution-sample spectrum, we note the very close similarities between the spectra displayed in Figure 2a,b. The spectrum shown in Figure 2c is that obtained for a 1:3 [Eu^{3+}]:[DPA] aqueous solution sample with [Eu^{3+}] = 0.10 M and pH = 8.5. Of special note in this

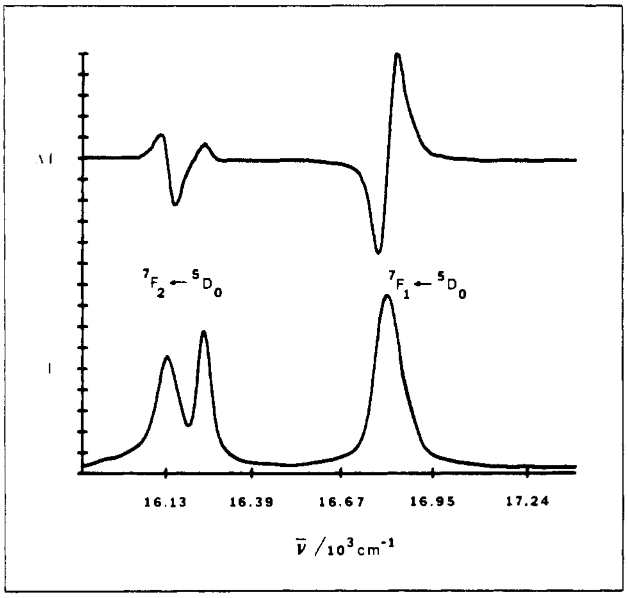

Figure 4. MCPL (ΔI) and total luminescence (I) spectra for 1:3 [Eu^{3+}]:[ODA] in aqueous solution at pH 9.0 ([Eu^{3+}] = 0.10 M, $|\mathbf{B}|$ = 4.2 T, and λ_{ex} = 466 nm).

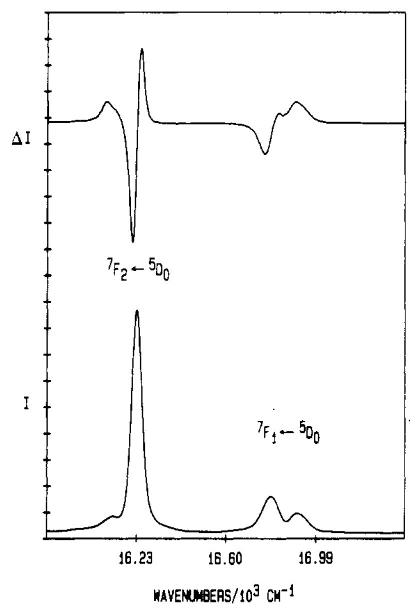

Figure 5. MCPL (ΔI) and total luminescence (I) spectra for 1:3 [Eu^{3+}]:[DPA] in aqueous solution at pH 8.5 ([Eu^{3+}] = 0.10 M, $|\mathbf{B}|$ = 4.2 T, and λ_{ex} = 466 nm).

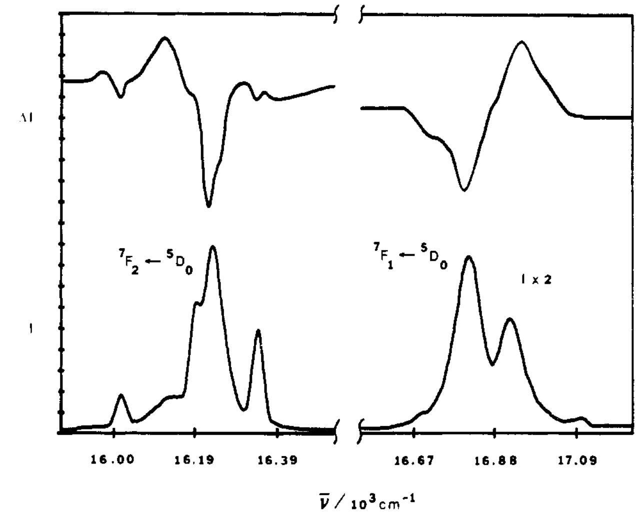

Figure 6. MCPL (ΔI) and total luminescence (I) spectra for 1:5 [Eu^{3+}]:[IDA] in aqueous solution at pH 8.5 ([Eu^{3+}] = 0.10 M, $|\mathbf{B}|$ = 4.2 T, and λ_{ex} = 466 nm).

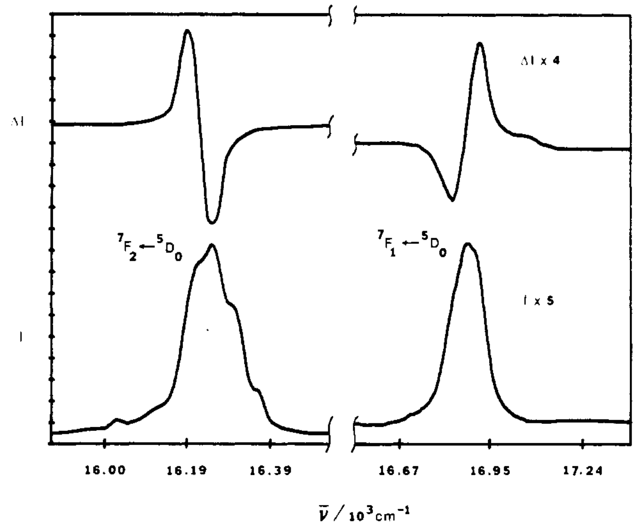

Figure 7. MCPL (ΔI) and total luminescence (I) spectra for 1:5 [Eu^{3+}]:[MIDA] in aqueous solution at pH 8.5 ([Eu^{3+}] = 0.10 M, $|\mathbf{B}|$ = 4.2 T, and λ_{ex} = 466 nm).

spectrum is the overwhelming dominance of the $^7F_2 \leftarrow {}^5D_0$ emission.

Emission spectra obtained on 1:5 [Eu^{3+}]:[IDA] and 1:5 [Eu^{3+}]:[MIDA] aqueous solution samples are shown in Figure 3. These spectra were obtained on samples with [Eu^{3+}] = 0.10 M and pH ~ 8.5–9.0. Again we note the dominance of $^7F_2 \leftarrow {}^5D_0$ emission.

Emission Spectra in an Applied Magnetic Field. MCPL (ΔI) and total luminescence (I) spectra, obtained in a magnetic field of $|\mathbf{B}|$ = 4.2 T, are shown in Figures 4–7 for the $^7F_{1,2} \leftarrow {}^5D_0$ transition regions. The total luminescence spectra shown in Figures 4, 5, and 7 for the ODA, DPA, and MIDA complexes, respectively, are qualitatively quite similar to the corresponding zero-field spectra presented in Figures 2 and 3. Although certain features in these spectra show field-induced broadening, none show any field-induced splittings. On the other hand, the MCPL spectra obtained for these complexes (the upper traces in Figures 4, 5, and 7) show quite clearly the magnetic sublevels of the $^7F_1$ and $^7F_2$ multiplets that are radiatively coupled to the $^5D_0$ emitting state. The total luminescence spectrum shown in Figure 6 for the IDA complex differs, qualitatively and quantitatively, from the corresponding zero-field spectrum in the $^7F_2 \leftarrow {}^5D_0$ transition region (see Figure 3). None of the systems examined in this study produced a measurable $^7F_0 \leftarrow {}^5D_0$ MCPL signal.

Discussion

Zero-Field Unpolarized Emission Intensities. To a very good approximation, the oscillator strength of the predominantly magnetic dipole $^7F_1 \leftarrow {}^5D_0$ transition is expected to be relatively independent of the ligand environment.[4,5] On the other hand, it is expected that the oscillator strength of the predominantly electric dipole $^7F_2 \leftarrow {}^5D_0$ transition will be extraordinarily sensitive to the ligand environment.[1-5] Therefore, observed variations in the $I(^7F_2 \leftarrow {}^5D_0):I(^7F_1 \leftarrow {}^5D_0)$ ratios, where I denotes total emission intensity, can be attributed largely to ligand perturbations on the $^7F_2 \leftarrow {}^5D_0$ electric dipole strengths. Among the systems examined in this study, the $I(^7F_2 \leftarrow {}^5D_0):I(^7F_1 \leftarrow {}^5D_0)$ ratio is observed to be smallest for $EuCl_3$ in water and largest for Eu(DPA). This observation correlates closely with what would be predicted from the ligand polarization model for lanthanide 4f → 4f electric dipole intensities. According to this model,[1,3,4,21,22] electric quadrupole allowed transitions (such as $^7F_2 \leftarrow {}^5D_0$) can acquire significant electric dipole strength via a quadrupole (Ln^{3+})-induced dipole (ligand) coupling mechanism, wherein the induced dipoles on the ligands are created by direct coupling to the electric dipolar components of the radiation field. By this mechanism, the 4f $\rightarrow$ 4f electric dipole strength should be related directly to ligand dipolar polarizabilities *and* to the anisotropies of these polarizabilities.[22,23] Clearly, among the ligands represented in this study, water molecules would present the least polarizable environment to the Eu^{3+} ion while the DPA ligands would be the most polarizable (due, primarily, to their pyridyl moiety).

Eu(ODA) Spectra. First we note the close similarities between the unpolarized emission spectra obtained for microcrystalline samples of $Na_3[Eu(ODA)_3]\cdot 2NaClO_4\cdot 6H_2O$ (Figure 2a) and for 1:3 [Eu^{3+}]:[ODA] in aqueous solution (Figure 2b). This immediately suggests that the dominant Eu(ODA) species present in solution is the tris-terdentate $Eu(ODA)_3{}^{3-}$ complex. In the solid state, this complex has trigonal dihedral (D_3) symmetry.[9,10] Orthoaxial linearly polarized emission studies on single crystals of $Na_3[Eu(ODA)_3]\cdot 2NaClO_4\cdot 6H_2O$ show that the A_2 and E components of the $^7F_1$ multiplet are only split by about 16 cm^{-1}, with the E level lying lowest in energy.[24] This corresponds to a value of $\sim$10.7 cm^{-1} for the $\Delta_1(2,0)$ quantity introduced in eq 7 and 8. This splitting is too small to be resolved in the room-temperature, isotropic spectra shown in Figure 2.

The MCPL spectrum shown in Figure 4 for the 1:3 Eu^{3+}/ODA system in aqueous solution conforms exactly to that predicted for a complex of trigonal dihedral (D_3) symmetry. Only one emission band is resolved in the $^7F_1 \leftarrow {}^5D_0$ transition region, but this band exhibits a slight asymmetry on its high-energy side. This suggests that the $A_2 \leftarrow A_1$ crystal field transition lies at slightly higher energy than the $E \leftarrow A_1$ transition and that $\Delta_1(2,0) \lesssim 0$ (opposite in sign to that observed for Eu^{3+} in the $Na_3[Eu(ODA)_3]\cdot 2NaClO_4\cdot 6H_2O$ system). With $\nu_{10}(E \leftarrow A_1) \approx \nu_{00}(A_2 \leftarrow A_1)$, one expects to see just a single *A* term in the $^7F_1 \leftarrow {}^5D_0$ MCPL spectrum, and this is precisely what is observed (see Figure 4). The observed *A* term is positive (meaning that ΔI goes from <0 to >0 as $\bar{\nu}$ increases), and from eq 16 we see that this requires that $\bar{A}_1(1 \leftarrow 0) > 0$.

Two emission bands are observed in the $^7F_2 \leftarrow {}^5D_0$ transition region, and these are assigned as $E_a \leftarrow A_1$ (at $\sim$16 240 cm^{-1}) and $E_b \leftarrow A_1$ (at $\sim$16 130 cm^{-1}). The *positive A* term observed in the $E_a \leftarrow A_1$ MCPL indicates that the E_a state has predominantly $M_J = \pm 1$ character, whereas the *negative A* term observed in the $E_b \leftarrow A_1$ MCPL indicates that the E_b state has predominantly $M_J = \pm 2$ character.

Eu(DPA) Spectra. One expects the dominant species in a 1:3 [Eu^{3+}]:[DPA] aqueous solution at pH >8 to be the tris-terdentate $Eu(DPA)_3{}^{3-}$ complex. Furthermore, from crystallographic studies[11-14] one expects this complex to have trigonal dihedral (D_3) symmetry. The emission spectrum shown in Figure 2c is compatible with this picture, if one assigns the higher energy $^7F_1 \leftarrow {}^5D_0$ emission band to an $A_2 \leftarrow A_1$ crystal field component and the lower energy $^7F_1 \leftarrow {}^5D_0$ band to an $E \leftarrow A_1$ crystal field component. Theory predicts the $E \leftarrow A_1$ transition to be about twice as intense as the $A_2 \leftarrow A_1$ transition. Furthermore, it is expected that the trigonal splitting within the $^7F_1$ multiplet will be greater for $Eu(DPA)_3{}^{3-}$ than for $Eu(ODA)_3{}^{3-}$, due to the highly polarizable pyridyl moiety present in the DPA ligands.[19]

Turning to the MCPL spectra shown in Figure 5, we see that the $^7F_1 \leftarrow {}^5D_0$ MCPL can be fit exactly by use of eq 16 if $\bar{A}_1(1 \leftarrow 0) > 0$ and $\bar{B}_0(1 \leftarrow 0) > 0$. The $\Delta I > 0$ band centered at $\sim$16 912 cm^{-1} is assigned to the $A_2 \leftarrow A_1$ crystal field transition and is described by eq 13. The two MCPL bands lying at lower energies (in the $^7F_1 \leftarrow {}^5D_0$ emission region) are assigned to Zeeman components of the $E \leftarrow A_1$ crystal field transition and are described by eq 12. The difference between the $^7F_1 \leftarrow {}^5D_0$ MCPL spectra observed for Eu(ODA) vs. Eu(DPA) can be accounted for entirely in terms of the relative magnitudes of the axial splitting parameter, $\Delta_1(2,0)$. In Eu(ODA), $|\Delta_1(2,0)| < 10$ cm^{-1}, and the oppositely signed $E \leftarrow A_1$ and $A_2 \leftarrow A_1$ *B*-term contributions to the $^7F_1 \leftarrow {}^5D_0$ MCPL spectrum effectively cancel one another (see eq 16); therefore, the spectrum exhibits just a single *A* term. In the case of Eu(DPA), $\bar{\nu}(E \leftarrow A_1) = 16797$ cm^{-1} and $\bar{\nu}(A_2 \leftarrow A_1) = 16912$ cm^{-1}, leading to a value of -77 cm^{-1} for $\Delta_1(2,0)$. In this case, the positively signed $A_2 \leftarrow A_1$ *B*-term contribution to the MCPL is clearly resolved (centered at 16 912 cm^{-1}), and the $E \leftarrow A_1$ MCPL exhibits superimposed *A* and *B* terms (centered at $\sim$16 797 cm^{-1}).

The $^7F_2 \leftarrow {}^5D_0$ emission region of Eu(DPA) exhibits a very intense line centered at $\sim$16 230 cm^{-1} and a weak feature centered at $\sim$16 132 cm^{-1}. We assign the former to the $E_a \leftarrow A_1$ crystal field transition and the latter (weak feature) to the $E_b \leftarrow A_1$ crystal field transition. The MCPL associated with the $E_a \leftarrow A_1$ transition exhibits a *positive A* term superimposed on a negatively signed *B* term, with the *A* term dominant. On the other hand, the MCPL observed in the $E_b \leftarrow A_1$ transition region appears to be dominated by a positively signed *B* term, with only a weak (*negative*) *A*-term component. This suggests that the $E_a \leftarrow A_1$ transition has predominantly $\Delta M_J = \pm 1$ character, whereas the $E_b \leftarrow A_1$ transition has predominantly $\Delta M_J = \pm 2$ character.

Eu(IDA) and Eu(MIDA) Spectra. At 1:5 [Eu^{3+}]:[ligand] concentration ratios and with solution pH >8, the dominant coordination species for Eu(IDA) and Eu(MIDA) are predicted to be the tris-terdentate complexes, $Eu(IDA)_3{}^{3-}$ and $Eu(MIDA)_3{}^{3-}$.[17,18] Furthermore, these complexes are expected to have approximate C_{3h} symmetry (see a discussion of this point in the Introduction). In C_{3h} symmetry, the crystal field components of the $J = 0$, 1, and 2 multiplets have the following symmetries (denoted by C_{3h} irreps): $J = 0$, A′; $J = 1$, A′ and E″; $J = 2$, A′, E′, and E″. For crystal field transitions originating from an A′ level (as in $^5D_0$), A′ ← A′ and E″ ← A′ are magnetic dipole allowed by crystal field selection rules and A″ ← A′ and E′ ← A′ are electric dipole allowed. From these selection rules, one predicts the following for the $^7F_{0,1,2} \leftarrow {}^5D_0$ emission spectra: $^7F_0 \leftarrow {}^5D_0$, a single magnetic dipole line (A′ ← A′); $^7F_1 \leftarrow {}^5D_0$, two magnetic dipole lines (A′ ← A′ and E″ ← A′); and $^7F_2 \leftarrow {}^5D_0$, two magnetic dipole lines (A′ ← A′ and E″ ← A′) and one electric dipole line (E′ ← A′). Intermediate-coupling selection rules (applicable to ΔJ), however, suggest that the magnetic dipole lines associated with the $^7F_{0,2} \leftarrow {}^5D_0$ transitions will be very weak. These lines can acquire intensity only to *at least* first order in H_{cf}^{+}.

The MCPL spectra shown in Figure 7 for Eu(MIDA) conform almost exactly to what is predicted for a C_{3h} complex. Only the very weak feature appearing at $\sim$17 060 cm^{-1} deviates from C_{3h} behavior. On the other hand, the MCPL spectra shown in Figure 6 for Eu(IDA) differ significantly from that predicted for C_{3h} systems. The latter results suggest significant concentrations of lower symmetry species in the 1:5 Eu^{3+}/IDA samples. This is most likely due to one or both of the following: (1) the formation of "outer-sphere" complexes via interactions between bound >N–H groups and some of the excess IDA ligands and (2) *partial* deprotonation of the bound >N–H groups under the pH conditions used in this study. Both of these possibilities would, of course, serve to differen-

(21) Mason, S. F.; Peacock, R. D.; Stewart, B. *Mol. Phys.* **1975**, *30*, 1829.
(22) Mason, S. F. *Struct. Bonding (Berlin)* **1980**, *39*, 43.
(23) Reid, M. F.; Richardson, F. S. *Chem. Phys. Lett.* **1983**, *95*, 501.
(24) Morley, J. P.; Saxe, J. D.; Richardson, F. S. *Mol. Phys.* **1982**, *47*, 379.

tiate between the complexation behaviors of MIDA and IDA.

Conclusions

The *relative* intensities observed among the $^7F_J \leftarrow {}^5D_0$ transitions in the unpolarized emission spectra reported in this study demonstrate the "hypersensitivity" of the $^7F_2 \leftarrow {}^5D_0$ transition to the ligand environment. Relative to the $^7F_1 \leftarrow {}^5D_0$ transition, this transition is most intense for the 1:3 Eu^{3+}/DPA system and least intense for $EuCl_3$ in water. This result supports the prediction of the ligand polarization model for hypersensitivity,[21,22] which states that the intensity of a hypersensitive transition should correlate with the dipolar polarizability of the ligand environment. Among the ligands examined in this study, DPA contains the most polarizabile group (the pyridyl moiety) while H_2O is the least polarizable.

The nearly identical unpolarized emission spectra obtained for microcrystalline $Na_3[Eu(ODA)_3]\cdot 2NaClO_4\cdot 6H_2O$ and 1:3 Eu^{3+}/ODA in aqueous solution suggest that the dominant species in solution is $Eu(ODA)_3^{3-}$, a tris-terdentate complex having trigonal dihedral (D_3) symmetry. The $^7F_{1,2} \leftarrow {}^5D_0$ MCPL spectra observed for the 1:3 Eu^{3+}/ODA solution samples are entirely compatible with such a structure. In fact, these spectra provide a near "textbook" example of what one expects for an axially symmetric Eu(III) complex in which the $h^+(2,0)$ component of the crystal field is relatively weak. The MCPL/emission spectra observed for the 1:3 Eu^{3+}/DPA system also conform exactly to that predicted for complexes of trigonal dihedral (D_3) symmetry. In this case, however, the $^7F_1 \leftarrow {}^5D_0$ MCPL/emission results reveal a relatively strong $h^+(2,0)$ crystal field component. The MCPL spectra obtained for the 1:5 Eu^{3+}/MIDA solution samples are identical with those predicted for a complex having C_{3h} symmetry, and the absence of any observed splitting within the $^7F_1 \leftarrow {}^5D_0$ transition region in the unpolarized spectra suggests a relatively weak $h^+(2,0)$ crystal field component. These results indicate that tris-terdentate $Eu(MIDA)_3^{3-}$ complexes of C_{3h} symmetry are the dominant species present in the 1:5 Eu^{3+}/MIDA solution samples.

Among the systems investigated in this study, only 1:5 Eu^{3+}/IDA in aqueous solution gave MCPL results suggesting the dominance of nonaxially symmetric structures. Given the $[Eu^{3+}]$:[IDA] concentration ratio (1:5) and pH conditions used in this study, it is likely that the dominant coordination species is $Eu(IDA)_3^{3-}$. However, in this case each bound IDA ligand possesses a >N–H group that is capable of promoting outer-sphere coordination to excess (unbound) ligands in solution. Since these outer-sphere complexes would be expected, in general, to possess nonaxially symmetric structures, it may be postulated that they account for the observed MCPL behavior of the 1:5 Eu^{3+}/IDA system.

It is clear that MCPL spectra can provide structural information not readily obtainable by the use of other techniques. Most previous applications of MCPL have been in studies of ions in crystals at low temperatures.[25–28] However, the results reported here demonstrate that it can also be used to great advantage in the study of lanthanide complexes in solution media at room temperature.

Acknowledgment. This work was supported by the National Science Foundation (NSF Grant CHE80-04209).

Registry No. $(ODA)_3^{3-}$, 43030-81-5; $Eu(DPA)_3^{3-}$, 38721-36-7; $Eu(IDA)_3^{3-}$, 87727-55-7; $Eu(MIDA)_3^{3-}$, 87682-22-2; $EuCl_3$, 10025-76-0.

(25) Morley, J. P.; Faulkner, T. R.; Richardson, F. S. *J. Chem. Phys.* **1982**, *77*, 1710.
(26) Morley, J. P.; Faulkner, T. R.; Richardson, F. S.; Schwartz, R. W. *J. Chem. Phys.* **1982**, *77*, 1734.
(27) Schwartz, R. W.; Brittain, H. G.; Riehl, J. P.; Yeakel, W.; Richardson, F. S. *Mol. Phys.* **1977**, *34*, 361.
(28) Luk, C. K.; Yeakel, W. C.; Richardson, F. S. *Chem. Phys. Lett.* **1975**, *34*, 147.

Contribution from the Departments of Chemistry, University of Virginia, Charlottesville, Virginia 22901, and Virginia Commonwealth University, Richmond, Virginia 23298

Magnetic Circularly Polarized Luminescence Spectra of Eu(β-diketonate)$_3$X$_2$ Complexes in Nonaqueous Solution

DAVID R. FOSTER,† F. S. RICHARDSON,*† L. M. VALLARINO,‡ and DONALD SHILLADY‡

Received January 14, 1983

Unpolarized emission spectra and magnetic field induced circularly polarized emission spectra are reported for $EuCl_3$ and for five different tris(β-diketonate) Eu(III) complexes in methanol and in *N,N*-dimethylformamide solutions. Analysis of the $EuCl_3$ spectra suggests the predominance of *axially* symmetric coordination species with C_{3v} point-group symmetry. Analysis of the tris(β-diketonate) Eu(III) spectra show the predominance of *nonaxially* symmetric structures with very strong orthorhombic crystal field components. The observed $^7F_2 \leftarrow {}^5D_0$ and $^7F_1 \leftarrow {}^5D_0$ emission intensity ratios exhibit a strong sensitivity to the structural details and chemical nature of the ligand environment, with the magnitude of $I(^7F_2 \leftarrow {}^5D_0):I(^7F_1 \leftarrow {}^5D_0)$ correlating closely with ligand or ligand substituent polarizabilities. The latter is explained in terms of the ligand dipolar polarization model for 4f → 4f electric dipole intensities. The $^7F_0 \leftarrow {}^5D_0$ transition intensity (relative to that of $^7F_1 \leftarrow {}^5D_0$) is also observed to be very sensitive to the ligand environment, and this is attributed to its "stealing" intensity from the $^7F_2 \leftarrow {}^5D_0$ transition via a mechanism involving crystal field induced mixings between the $^7F_0$ and $^7F_2$ (and $^5D_0$ and $^5D_2$) multiplet states.

Introduction

In the preceding paper,[1] we reported magnetic circularly polarized luminescence (MCPL) spectra obtained on four different Eu^{3+}–ligand systems that, in aqueous solution under basic conditions, were shown to form predominantly tris-terdentate (9-coordinate) complexes with trigonal symmetry (either D_3 or C_{3h}). In the present paper, we report MCPL spectra for a series of 8-coordinate Eu(β-diketonate)$_3$X$_2$ complexes dissolved in either methanol (MeOH) or *N,N*-dimethylformamide (DMF). In this series, the β-diketonate ligands differ with respect to their substituent groups and X represents either a water molecule or a solvent molecule

† University of Virginia.
‡ Virginia Commonwealth University.

(1) Foster, D.; Richardson, F. S. *Inorg. Chem.*, preceding paper in this issue.

